



**HAL**  
open science

## Normalised Stiffness Ratios for Mechanical Characterization of Isotropic Acoustic Foams

Sohbi Sahraoui, Bruno Brouard, Lazhar Benyahia, Damien Parmentier, Alan  
Geslain

► **To cite this version:**

Sohbi Sahraoui, Bruno Brouard, Lazhar Benyahia, Damien Parmentier, Alan Geslain. Normalised Stiffness Ratios for Mechanical Characterization of Isotropic Acoustic Foams. *Journal of the Acoustical Society of America*, 2013, 134 (6), pp.4624-4629. 10.1121/1.4824833 . hal-02638951

**HAL Id: hal-02638951**

**<https://hal.science/hal-02638951v1>**

Submitted on 29 Aug 2024

**HAL** is a multi-disciplinary open access archive for the deposit and dissemination of scientific research documents, whether they are published or not. The documents may come from teaching and research institutions in France or abroad, or from public or private research centers.

L'archive ouverte pluridisciplinaire **HAL**, est destinée au dépôt et à la diffusion de documents scientifiques de niveau recherche, publiés ou non, émanant des établissements d'enseignement et de recherche français ou étrangers, des laboratoires publics ou privés.



Distributed under a Creative Commons Attribution - NonCommercial 4.0 International License

# Normalized stiffness ratios for mechanical characterization of isotropic acoustic foams

Sohbi Sahraoui<sup>a)</sup> and Bruno Brouard

LAUM, CNRS UMR 6613, Université du Maine, Avenue O. Messiaen, 72085 Le Mans, France

Lazhar Benyahia

PCI, CNRS UMR 6120, Université du Maine, Avenue O. Messiaen, 72085 Le Mans, France

Damien Parmentier

CTTM, Centre de Transfert de Technologie, 20 rue Thalès de Milet, 72000, Le Mans, France

Alan Geslain

LAUM, CNRS UMR 6613, Université du Maine, Avenue O. Messiaen, 72085 Le Mans, France

This paper presents a method for the mechanical characterization of isotropic foams at low frequency. The objective of this study is to determine the Young's modulus, the Poisson's ratio, and the loss factor of commercially available foam plates. The method is applied on porous samples having square and circular sections. The main idea of this work is to perform quasi-static compression tests of a single foam sample followed by two juxtaposed samples having the same dimensions. The load and displacement measurements lead to a direct extraction of the elastic constants by means of normalized stiffness and normalized stiffness ratio which depend on Poisson's ratio and shape factor. The normalized stiffness is calculated by the finite element method for different Poisson ratios. The no-slip boundary conditions imposed by the loading rigid plates create interfaces with a complex strain distribution. Beforehand, compression tests were performed by means of a standard tensile machine in order to determine the appropriate pre-compression rate for quasi-static tests.

## I. INTRODUCTION

Sound propagation in open cell foams can be described by the phenomenological Biot theory<sup>1,2</sup> which requires the knowledge of the viscoelastic properties of the solid phase. The concept of complex modulus is widely used in acoustics to characterize the dynamic elastic and damping properties of solid materials in the linear range. However, numerous works propose more adapted approaches like the fractional derivatives model<sup>3</sup> and a monograph is also dedicated to the fractional calculation in viscoelasticity.<sup>4</sup>

To characterize the viscoelastic properties of acoustic foams, only a few experimental techniques are available in the literature including non-resonant techniques,<sup>5-7</sup> standing wave resonance of a longitudinally excited rod with end mass,<sup>8,9</sup> or mass-spring resonance.<sup>10</sup> All these methods are suited for measurements in a narrow frequency range. An extension of these measurement techniques for a wider frequency range has been made using theoretical modeling of foams viscoelastic behavior,<sup>11</sup> through the frequency-temperature superposition principle,<sup>12</sup> or by means of acoustic excitations.<sup>13,14</sup>

Due to the manufacturing process, porous materials, such as foamed polymers, exhibit highly anisotropic elastic properties. In the rising direction, non-regular cell geometry

is induced which, in general, leads to highly directive cell orientations. Since Biot's contribution,<sup>15</sup> numerous works were reported in the literature on the anisotropy of geo-materials.<sup>16,17</sup> However, the acoustic materials studied after the Biot-Johnson-Allard theory<sup>2</sup> benefit especially from numerical investigations.<sup>18,19</sup> More recently, Cuenca and Goransson<sup>20</sup> present a numerical methodology for the inverse estimation of the elastic and anelastic parameters of orthotropic porous sample having a cubic form. Experimentally, strength and stiffness are found to be higher in the direction of the elongated cells.<sup>21-23</sup> In particular, Guastavino and Göransson<sup>21</sup> and Guastavino<sup>24</sup> reported a mapping of the three-dimensional full-field displacement and showed a complex strain on the four free faces due to foam anisotropy and the boundary conditions; a methodology for identification of general orthotropic elastic models of porous foams is proposed. The lack of experimental investigations for accessing viscoelastic properties of anisotropic polymeric foams is connected to problems of measurements and to the nature of these materials. Some works perform an experimental investigation on anisotropic tortuosity,<sup>25</sup> flow resistivity,<sup>22,26,27</sup> and introduce shear modulus in two planes.<sup>28</sup> The present contribution is focused on selected isotropic samples.

In the work by Mariez *et al.*<sup>5</sup> a cubic foam sample is compressed between two horizontal rigid plates. The Young modulus  $E$  and the Poisson's ratio  $\nu$  are adjusted using a static finite element model of the test setup to match the measured mechanical impedance. This method requires the

---

<sup>a)</sup>Author to whom correspondence should be addressed. Electronic mail: sohbi.sahraoui@univ-lemans.fr

measure of the lateral displacement of one vertical face center by a laser vibrometer. The method described in the present paper does not require the laser vibrometer; instead, the stiffness in compression is measured in two configurations: One brick-shaped sample having a square section and two juxtaposed identical samples. The calculations were performed for some shape factors and Poisson's ratios (0 to 0.48 by 0.005 step). The shape factor is defined as the side of the square section to the thickness ratio. The main approach to test two identical samples on top of each other gives a straightforward access to  $E$  and  $\nu$  by means of the introduction of the normalized stiffness ratio. The extraction of these elastic constants is simpler than the procedure by Langlois *et al.*<sup>7</sup> which uses polynomial relations for cylindrical samples. The investigation of cubic samples has allowed the selection of quasi-isotropic foam samples.

The elastic and static compression is simulated by the finite element method in Sec. II: Calculations of normalized stiffness and normalized stiffness ratio have been performed for parallelepipedic and cylindrical samples. Section III is focused on the mechanical behavior of the foams in static compression by means of a standard tensile machine; an experimental procedure was developed for analyzing the load-displacement curves, the spatial dispersion of the stiffness, and the validation of the sample juxtaposition method. Finally, quasi-static characterization results at a chosen frequency are presented and discussed with some recommendations in Sec. IV.

## II. FINITE ELEMENT SIMULATION OF STATIC COMPRESSION

Static and quasi-static compression tests are performed in Sec. II A on parallelepipedic and cylindrical samples as shown in Fig. 1 where  $F$  and  $\nu$  represent the measured load and displacement. The stiffness  $K$  defined by

$$K = F/\nu, \quad (1)$$

is dependent on Young modulus and Poisson's ratio for a given sample. This section is devoted to the finite element simulation of these tests for extracting the elastic constants of investigated foams.

### A. Parallelepipedic samples

For parallelepipedic samples having a square section ( $A=L^2$ ) and a thickness  $h$  the shape factor  $s$  is defined as  $L/h$ . The stiffness  $K_s$ , defined by Eq. (1) for a shape factor  $s$ ,

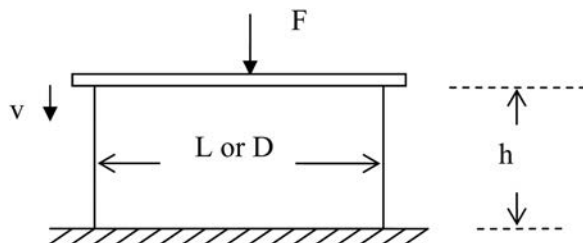


FIG. 1. Sample in static compression.

depends on the elastic constants and the sample dimensions and can be written as<sup>5,6</sup>

$$K_s = \frac{EA}{h} k_s(\nu) = \frac{EA}{L/s} k_s(\nu), \quad (2)$$

where  $k_s$  is the normalized stiffness.

For a half parallelepipedic sample (with the thickness and the shape factor equal to  $h/2$  and  $2s$ , respectively), the stiffness is defined by the following equation:

$$K_{2s} = \frac{EA}{L/2s} k_{2s}(\nu), \quad (3)$$

where  $k_{2s}$  is the normalized stiffness. Finite element simulations are performed in order to compute the normalized stiffness for different combinations of Poisson's ratio and shape factor.

By using Eqs. (2) and (3) the normalized stiffness ratio  $\alpha_s$ , defined as  $k_s/k_{2s}$ , can be obtained in the following form:

$$\alpha_s(\nu) = \frac{k_s}{k_{2s}} = \frac{2K_s}{K_{2s}}, \quad (4)$$

where the ratio  $K_s/K_{2s}$  is only dependent on Poisson's ratio. The normalized stiffness  $k_s$  and the ratio  $\alpha_s(\nu)$  are plotted in Figs. 2 and 3. It can be observed that  $k_s$  values are close to 1 for low Poisson's ratio; in this case the simulation confirms that the sample does not bulge sideways as observed by laser vibrometer measurements in a previous study.<sup>5</sup>

The function  $\alpha_s(\nu)$  plotted in Fig. 3 gives a straightforward access to  $E$  and  $\nu$  in the following way. In this method, the two elastic constants are easily calculated in two steps:

- (1) The normalized stiffness ratio  $\alpha_s$  gives  $\nu$  by using the data in Fig. 3;
- (2) the  $\nu$  value calculated above yields  $k_s$  through Fig. 2 and then the Young's modulus is determined from the measured stiffness and Eq. (2) as

$$E = \frac{K_s}{sLk_s(\nu)}. \quad (5)$$

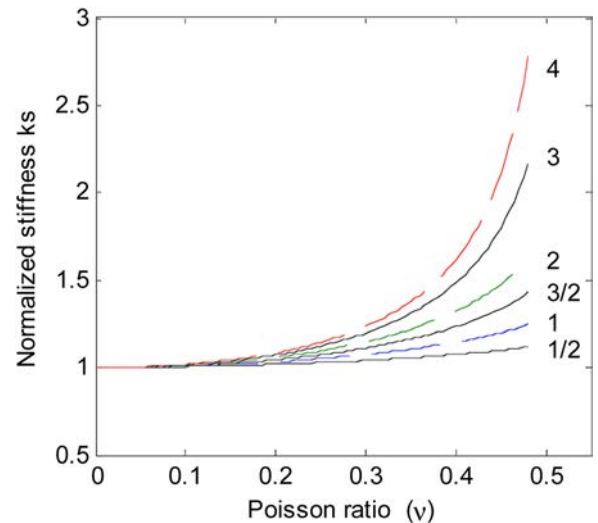


FIG. 2. (Color online) Numerical stiffness as a function of Poisson's ratio for various shape ratios of parallelepipedic samples.

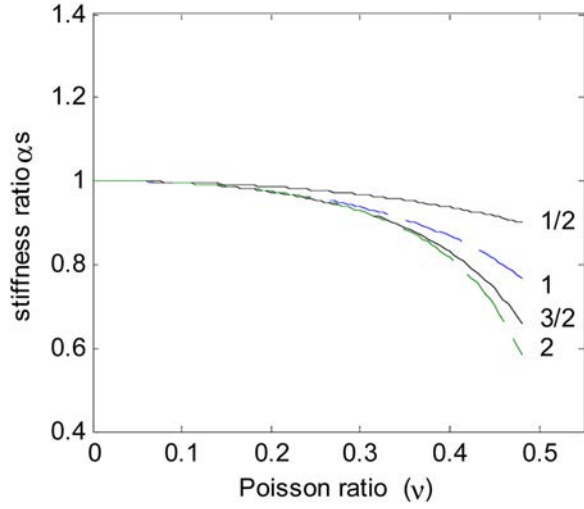


FIG. 3. (Color online) Normalized stiffness ratio as a function of Poisson's ratio for parallelepipedic samples.

This procedure is summarized in Fig. 4. Using the  $\alpha_s(\nu)$  curve, the measured value  $a = K_s/K_{2s}$  is related to the corresponding value  $b$  of  $\nu$  [Eq. (4)] and then the value  $c$  of the normalized stiffness  $k$  is obtained. Finally, the measured stiffness  $K_s$  and Eq. (5) allow the determination of  $E$ . This extraction method of elastic constants allows displaying the errors of measurements according to the shape factor  $s$ ; for instance, we can reduce the error  $\Delta\nu$  with samples having a large  $s$ .

### B. Cylindrical samples

The method developed for brick-shaped samples can be extended to disk-shaped samples with the shape factor  $s$  defined as  $D/h$ , where  $D$  is the sample diameter. Then Eq. (2) takes the same form

$$K_s = \frac{EA}{D/s} k'_s(\nu). \quad (6)$$

Similarly we can numerically compute a new normalized stiffness  $k'_s$  and stiffness ratio  $\alpha'_s$  as explained above for

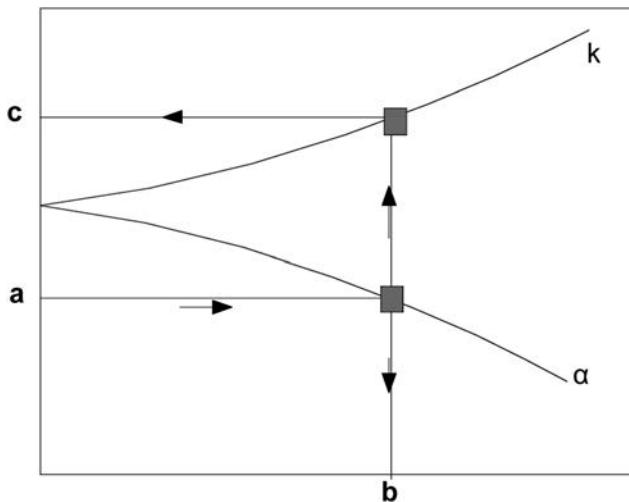


FIG. 4. Graphical representation of the procedure to obtain  $\nu$  and  $E$  by using  $\alpha$  and  $k$  curves ( $a \rightarrow b \rightarrow c$ ).

parallelepipedic samples. Therefore the experimental values of  $K_s$  and  $K_{2s}$  can be used to calculate first  $\nu$  through  $\alpha'_s$  as

$$\alpha'_s(\nu) = \frac{k'_s}{k'_{2s}} = \frac{2K_s}{K_{2s}}, \quad (7)$$

and second  $E$  using Eq. (6).

The normalized stiffness and the normalized stiffness ratio (Fig. 5) are calculated for the shape factors of the samples tested in Sec. IV.

### III. STATIC COMPRESSION TESTS

The parallelepipedic samples were usually cut with a high speed rotating sharp blade. We obtain a nicer cutting with the water jet technique and a good parallelism of the loading surfaces. The plates are covered with sandpaper to prevent radial sliding at the sample-plate interfaces.

Preliminary compression tests were performed by means of a standard tensile machine where the crosshead speed was fixed at 10 mm/min. The objectives of these measurements were to study the mechanical behavior of the sample during loading and to select foam with properties close to that of a quasi-isotropic material. Furthermore, the validity of the sample superposition is investigated. As indicated below, the measured load and the crosshead displacement used for calculating the stiffness  $K$  [Eq. (1)] are denoted as  $F$  and  $\nu$ , respectively.

#### A. Evolution of the stiffness $K$

In static loading, the typical load-displacement curves plotted in Fig. 6 exhibit a first zone I where the slope ( $dF/d\nu$ ) is increasing and a second zone II having a linear elastic behavior. The no-slip boundary conditions imposed by the rigid plates during the beginning of the loading create interfaces with a complex strain distribution and shear stress where the collapse of the cells is followed by a static compression. In a deformation mapping study, Guastavino and Göransson<sup>21</sup> have observed a significant large gradient of the displacement near the loading plate which could confirm the

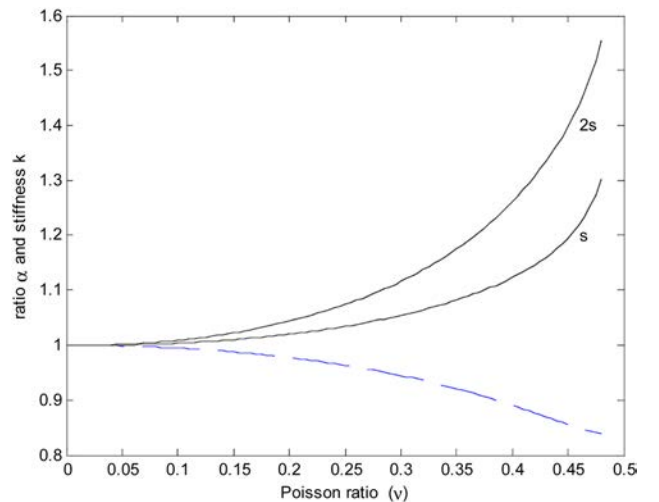


FIG. 5. (Color online) Normalized stiffness  $k'_s$ ,  $k'_{2s}$ , and stiffness ratio  $\alpha'_s$  (dotted line) for cylindrical samples ( $s = 1.1$ ).

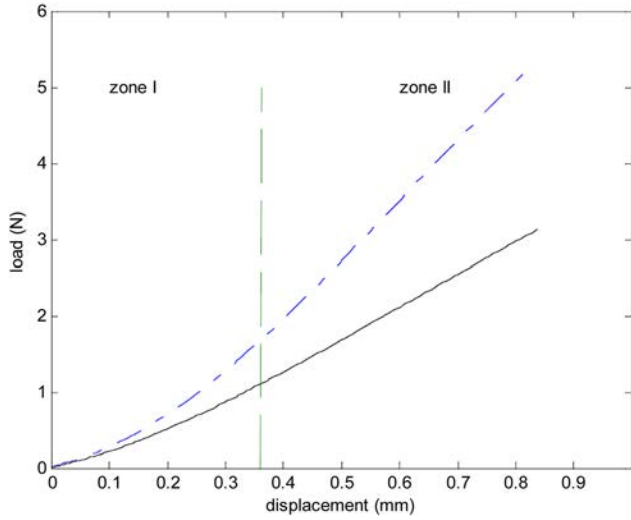


FIG. 6. (Color online) Static compression test for a cube and half cube (dotted line).

interface zones mentioned above. For cube (40 mm side) and half cube samples, the width of the zone is 0.36 mm (Fig. 6) then the thickness for each interface can be estimated as less than 0.18 mm. The first zone is governed by the interface process and presents an increase of the slope. The second zone corresponds to the compression state in the whole sample. The pre-strain rate must be chosen in this zone for quasi-static tests.

### B. Isotropic foams

Open-cell foams exhibit a quasi-axisymmetrical behavior<sup>22,24</sup> and the rising direction during the foaming process, named longitudinal direction, is orthogonal to the transverse isotropic plane.

As mentioned above, the cubic geometry allows us to check the isotropy or the degree of anisotropy by comparing the stiffness in the three directions. The commercially available plates are generally cut in the transverse plane defined here by  $T1$  and  $T2$  directions; the third rising direction is denoted as  $L$ . Four foams having a cubic geometry (40 mm side) were tested in their three orthogonal directions for measuring  $K_{T1}$ ,  $K_{T2}$ , and  $K_L$ . The selected foam has relative stiffness values of 100, 104, and 112, respectively, in the three directions; the assumption of isotropy involves 12% deviation for  $K_L$  while it can reach 80% for some foam.

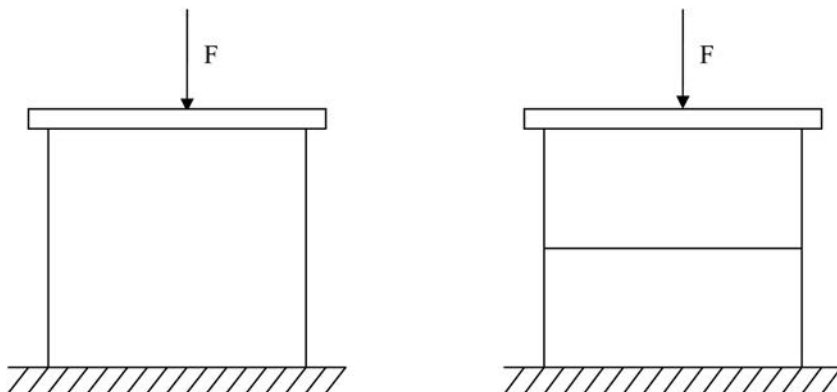


FIG. 7. Configuration of whole and juxtaposed samples in compression.

### C. Foam plate homogeneity

For characterizing the acoustic material, the approach presented in this paper requires two samples having the same dimensions. For a better knowledge of spatial dispersion of the foam plate properties, a static stiffness evaluation has been performed on both series of about 10 samples with the following dimensions:  $80 \times 80 \times 20 \text{ mm}^3$  and  $40 \times 40 \times 20 \text{ mm}^3$ . The resulting dispersions in the first and second series are 6% and 9%, respectively; as expected, the standard deviation is smaller for the large size samples.

### D. Validation of sample juxtaposition method

As mentioned before shear stress arises from the no-slip conditions at the loading surfaces. The absence of shear stress in the horizontal plane of symmetry of the samples is the basic property suggesting testing two juxtaposed samples (Fig. 7). Here, we attempt to show the validation of the proposed method for two shape factors ( $s=1$  and  $s=2$ ). First we compare the stiffness of the entire cubic samples cut in foam plate with thickness 40 mm and of two juxtaposed half cubes ( $40 \times 40 \times 20 \text{ mm}^3$ ). Second, this comparison is made also for another whole sample ( $80 \times 80 \times 40 \text{ mm}^3$ ) and two juxtaposed half samples ( $80 \times 80 \times 20 \text{ mm}^3$ ).

All tests on the whole samples and on two half samples give similar results with standard deviation in the range obtained in Sec. III C. The method described above is applied in Sec. IV to identical samples cut from the same foam plate; the stiffness measurements are performed on two juxtaposed samples and on one sample.

## IV. QUASI-STATIC MEASUREMENTS: RESULTS AND DISCUSSION

This section presents an example of the characterization procedure using previous normalized stiffness and normalized stiffness ratio defined in Eqs. (2), (3), and (4) for parallelepipedic samples; the same characterization is performed for cylindrical samples by using Eqs. (6) and (7). Section III highlighted the heterogeneity and the anisotropy of the acoustic foams as well as the existence of an interface zone. The validation of the method of juxtaposition of two samples and the determination of pre-strain rate are used for quasi-static tests in the range [0 to 100 Hz] and applied to the quasi-isotropic foam.



The polyurethane (PU) isotropic foam selected in Sec. III B is characterized in compression with the measurement setup depicted in Fig. 8 where the bottom plate is submitted to the harmonic displacement

$$v = v_0 + v_1 \sin \omega t, \quad (8)$$

where the relative displacement  $v_0/h$  and the relative amplitude  $v_1/h$  are fixed at 3% and 0.1%, respectively. In complex notation the bottom face of the sample has the displacement

$$\hat{v} = v_0 + v_1 e^{j\omega t}, \quad (9)$$

and the complex Young's modulus  $\hat{E}$  takes the form

$$\hat{E} = E(1 + j\eta), \quad (10)$$

where  $E$  and  $\eta$  represent the Young's modulus and the loss factor, respectively. The computer-controlled device is equipped with a displacement sensor.

Brick-shaped and disk-shaped samples are cut from a PU foam plate being 20 mm in thickness; for square ( $40 \times 40$  or  $80 \times 80$ ) and circular ( $D = 44$  mm) sections the shape factors are 2, 4, and 2.2, respectively. The measurements of identical sample stiffness show some fluctuation (6% to 9%) due to the foam heterogeneity. The results presented in Table I give the mean value. The influence of initial strain and frequency excitation on Young modulus and the relaxation effects of the polymer are discussed elsewhere.<sup>29</sup>

One major difficulty for the characterization of mechanical parameters of poroelastic material is the high sensitivity of these parameters to various experimental conditions. The quasi-static measurements described at the beginning of this section have been used in addition to the static investigation presented in Sec. III. For more accuracy in the experiments, the sample preparation and the experimental conditions such as sample cutting and geometrical imperfections and the choice

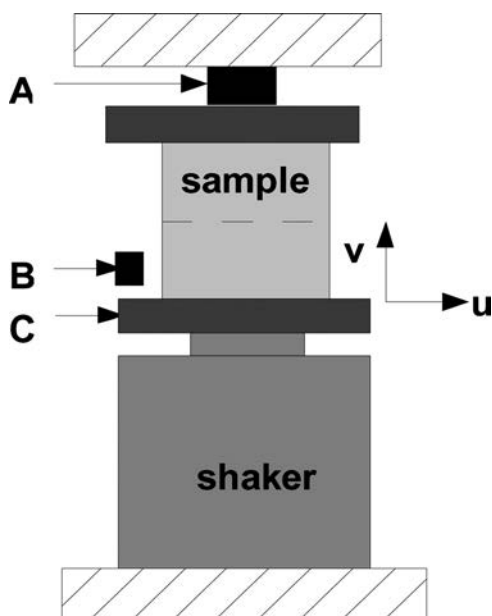


FIG. 8. Experimental setup (A: Load  $F$  sensor, B: Displacement  $v$  sensor of the moving plate C).

TABLE I. Mechanical parameters of the selected foam at 40 Hz and at room temperature (20 °C).

	Square section ( $40 \times 40$ mm <sup>2</sup> )	Square section ( $80 \times 80$ mm <sup>2</sup> )	circular section ( $D = 44$ mm)
$E$ (kPa)	$292 \pm 13$	$302 \pm 9$	$311 \pm 14$
$\nu$	$0.42 \pm 0.04$	$0.40 \pm 0.03$	$0.43 \pm 0.04$
$\eta$	$0.12 \pm 0.01$	$0.12 \pm 0.01$	$0.11 \pm 0.01$

of initial compression must be taken into account.<sup>24,30–32</sup> The use of the tensile machine is not indispensable but it is necessary to choose a correct initial relative displacement  $v_0/h$  to avoid measuring the stiffness in the zone I (Fig. 6). This figure shows the increase of the slope in zone I and a linear part with a constant value of slope in zone II where  $v_0$  can be chosen. Knowing that the foams have a transverse isotropy,<sup>22</sup> the stiffness measurements on a cubic sample give some information on the degree of anisotropy and allow the correct evaluations of the standard deviation. Numerous points approached in this work, such as anisotropy, heterogeneity, and experimental details, highlight the necessity of standardization on the characterization of polymeric acoustic foams. The influence of the coupling with fluid phase was not considered in the study because it is insignificant at low frequency.<sup>33,34</sup>

## V. CONCLUSION

In this paper, quasi-static measurements of acoustic foams were performed to determine the elastic properties of selected isotropic samples. The method uses two identical brick-shaped or disk-shaped samples cut from commercially available porous plates. The main originality lies in the development of a normalized stiffness ratio for a straightforward extraction of the Young's modulus and the Poisson's ratio. The developed method, which does not require polynomials inversion during the characterization process, is a simpler alternative. Preliminary static compression tests by means of a tensile machine allowed to validate the method of juxtaposition and to define the experimental conditions for the quasi-static measurements such as the pre-strain rate determination.

Furthermore this work highlights the spatial dispersion of foam plate's properties and the anisotropic behavior of these porous materials; the use of cubic samples is necessary for evaluating the degree of anisotropy and estimating the isotropy approximation. The characterization of anisotropic foams using the presented method is currently under development.

## ACKNOWLEDGMENTS

The authors would like to thank J.-F. Rondeau (FAURECIA) for his contribution in foam sample preparation. The authors are grateful to X. Guo and G. Yan for their critical remarks.

<sup>1</sup>M. A. Biot, "The theory of propagation of elastic waves in a fluid-saturated porous solid. I. Low frequency range. II. Higher frequency range," *J. Acoust. Soc. Am.* **28**, 168–191 (1956).

<sup>2</sup>J. F. Allard, *Propagation of Sound in Porous Media: Modeling Sound Absorbing Materials* (Elsevier Applied Science, London, 1993), pp. 1–279.

- <sup>3</sup>R. L. Bagley and P. J. Torvik, "On the fractional calculus model of viscoelastic behavior," *J. Rheol.* **30**, 133–155 (1986).
- <sup>4</sup>F. Mainardi, *Fractional Calculus and Waves in Linear Viscoelasticity* (Imperial College Press, London, 2010), Chap. 6, pp. 1–76.
- <sup>5</sup>E. Mariez, S. Sahraoui, and J. F. Allard, "Elastic constants of polyurethane foam's skeleton for Biot model," in *Proceedings of Internoise*, Budapest, Vol. 96, pp. 951–954 (1996).
- <sup>6</sup>S. Sahraoui, E. Mariez, and M. Etchessahar, "Mechanical testing of polymeric foams at low frequency," *Polym. Test.* **20**, 93–96 (2001).
- <sup>7</sup>C. Langlois, R. Panneton, and N. Atalla, "Polynomial relations for quasi-static mechanical characterization of isotropic poroelastic materials," *J. Acoust. Soc. Am.* **110**, 3032–3040 (2001).
- <sup>8</sup>T. Pritz, "Dynamics Young's modulus and loss factor of plastic foams for impact sound isolation," *J. Sound Vib.* **178**, 315–322 (1994).
- <sup>9</sup>A. Sfaoui, "On the viscoelasticity of polyurethane foams," *J. Acoust. Soc. Am.* **97**, 1046–1052 (1995).
- <sup>10</sup>T. Pritz, "Non-linearity of frame dynamic characteristics of mineral and glass wool materials," *J. Sound Vib.* **136**, 263–274 (1990).
- <sup>11</sup>T. Pritz, "Analysis of four-parameter fractional derivative model of real solid materials," *J. Sound Vib.* **195**, 103–115 (1996).
- <sup>12</sup>M. Etchessahar, S. Sahraoui, L. Benyahia, and J. F. Tassin, "Frequency dependence of elastic properties of acoustic foams," *J. Acoust. Soc. Am.* **117**, 1114–1121 (2005).
- <sup>13</sup>J. F. Allard, M. Henry, L. Boeckx, P. Leclaire, and W. Lauriks, "Acoustical measurement of the shear modulus for thin porous layers," *J. Acoust. Soc. Am.* **117**, 1737–1743 (2005).
- <sup>14</sup>V. Garetton, D. Lafarge, and S. Sahraoui, "The measurement of the shear modulus of a porous polymer layer with two microphones," *Polym. Test.* **28**, 508–510 (2009).
- <sup>15</sup>M. A. Biot, "Theory of elasticity and consolidation for a porous anisotropic solid," *J. Appl. Phys.* **26**, 182–185 (1955).
- <sup>16</sup>S. Crampin and Y. Gao, "A review of a quarter century of International Workshops on Seismic Anisotropy in the crust," *J. Seismol.* **13**, 181–208 (2009).
- <sup>17</sup>K. Helbig and L. Thomsen, "75th Anniversary Paper—75-plus years of anisotropy in exploration and reservoir seismics: A historical review of concepts and methods," *Geophysics* **70**, 9–23 (2005).
- <sup>18</sup>N.-E. Horlin and P. Goransson, "Weak, anisotropic symmetric formulations of Biot's equations for vibro-acoustic modeling of porous elastic materials," *Int. J. Numer. Methods Eng.* **84**, 1519–1540 (2010).
- <sup>19</sup>P. Goransson and N.-E. Horlin, "Vibro-acoustic modeling of anisotropic porous elastic materials: A preliminary study of the influence of anisotropy on the predicted performance in a multi-layer arrangement," *Acta. Acust. Acust.* **96**, 258–265 (2010).
- <sup>20</sup>J. Cuenca and P. Göransson, "Inverse estimation of the elastic and anelastic properties of the porous frame of anisotropic open-cell foams," *J. Acoust. Soc. Am.* **132**, 133–155 (1986).
- <sup>21</sup>R. Guastavino and P. Göransson, "A 3D displacement measurement methodology for anisotropic porous cellular foam materials," *Polym. Test.* **26**, 711–719 (2007).
- <sup>22</sup>M. Melon, E. Mariez, C. Ayrault, and S. Sahraoui, "Acoustical and mechanical characterization of anisotropic open-cell foams," *J. Acoust. Soc. Am.* **104**, 2622–2627 (1998).
- <sup>23</sup>E. Mariez and S. Sahraoui, "Measurement of mechanical anisotropic properties of acoustic foams for the Biot model," in *Proceedings of Internoise*, Vol. 97, pp. 1683–1686 (1997).
- <sup>24</sup>R. Guastavino, "Elastic and acoustic characterization of anisotropic porous materials," Ph.D. dissertation, KTH Engineering Science, Stockholm (2008).
- <sup>25</sup>M. Melon, D. Lafarge, B. Castagnede, and N. Brown, "Measurement of tortuosity of anisotropic acoustic material," *J. Appl. Phys.* **78**, 4929–4932 (1995).
- <sup>26</sup>B. Castagnede, A. Aknine, M. Melon, and C. Depollier, "Ultrasonic characterization of the anisotropic behavior of air-saturated porous materials," *Ultrasonics* **36**, 323–341 (1998).
- <sup>27</sup>P. Goransson, R. Guastavino, and N.-E. Horlin, "Measurement and inverse estimation of 3D anisotropic flow resistivity for porous materials," *J. Sound Vib.* **327**, 354–367 (2009).
- <sup>28</sup>P. Khurana, P. Leclaire, L. Boeckx, W. Lauriks, O. Dazel, and J. F. Allard, "A description of transversely isotropic sound absorbing porous materials by transfer matrices," *J. Acoust. Soc. Am.* **125**, 915–921 (2009).
- <sup>29</sup>A. Geslain, O. Dazel, J.-P. Groby, S. Sahraoui, and W. Lauriks, "Influence of static compression on mechanical parameters of acoustic foams," *J. Acoust. Soc. Am.* **130**, 818–825 (2011).
- <sup>30</sup>M. Etchessahar, "Low frequency mechanical characterization of acoustic materials," Ph.D. thesis, Université du Maine, Le Mans, France (2002).
- <sup>31</sup>L. Jaouen, A. Renault, and M. Deverge, "Elastic and damping characterization in acoustical porous materials: Available experimental methods and applications to a melamine foam," *Appl. Acoust.* **69**, 1129–1140 (2008).
- <sup>32</sup>L. Jaouen, "Contribution to the mechanical characterization of poroviscoelastic materials," Ph.D. thesis, Université du Maine, Le Mans, France (2003).
- <sup>33</sup>N. Dauchez, M. Etchessahar, and S. Sahraoui, "On measurement of mechanical properties of sound absorbing materials," in *Proceedings of Poromechanics II*, pp. 627–631 (2002).
- <sup>34</sup>O. Danilov, F. Sgard, and X. Olny, "On the limits of an 'in vacuum' model to determine the mechanical parameters of isotropic poroelastic materials," *J. Sound Vib.* **276**, 729–754 (2004).